The importance of weather and tides on the resuspension and deposition of microphytobenthos (MPB) on intertidal mudflats

Nurul Shahida Redzuan [a,b,*], Graham J.C. Underwood [a]

[a] School of Life Sciences, University of Essex, Colchester, CO4 3SQ, United Kingdom
[b] Faculty of Science and Marine Environment, Universiti Malaysia Terengganu, 21030, Kuala Terengganu, Terengganu, Malaysia

ARTICLE INFO

ABSTRACT

Abiotic variables, such as weather and tidal forces, are potentially as important as biotic factors (growth, predation, competition) in driving the variability of microphytobenthic (MPB) biomass on intertidal flats. Patterns of spatial distribution and temporal variability in MPB Chl. *a*, sediment Extracellular Polymeric Substances (EPS) and benthic diatom species composition were investigated during daily sampling spanning neap to spring tide periods on intertidal mudflats in the Colne Estuary, U.K., in three different seasons, with a particular focus on the influence of wind, rainfall, sun hours in the days prior to sampling, and tidal range. Spatial distribution (at < 1 m and <5 m scales) made the greatest contribution to biomass variability, followed by temporal (inter-monthly) variability. MPB Chl. *a* and EPS concentrations were positively correlated with sun-hours and tidal range, and negatively with rainfall and wind speed. Higher benthic MPB biomass was associated with lower suspended solid and Chl *a* loads, indicating biostabilisation of surface sediment. Suspended sediment loads and suspended Chl. *a* concentrations were positively correlated, and were significantly higher during neap rather than spring tides. Sediment settlement rates were higher during neap tides and related to suspended sediment load. The percent similarity in the benthic and suspended diatom assemblages (species relative abundance, RA) increased linearly with suspended solid load, with highest similarity during neap tides, with pennate benthic diatom taxa (*Gyrosigma balticum*, *G. scalproides* and *Pleurosigma angulatum*) dominant, indicating local sediment resuspension. During Spring tides, species similarity was lower, with a higher RA of planktonic centric diatoms (*Actinoptychus*, *Coscinodiscus* and *Odontella*) and lower sediment loads. Despite greater volumes of water movement during high tidal range periods, the highest levels of localised resuspension and remobilisation of MPB biomass across the mudflats occurred during low tidal range neap tide periods, when wind-induced waves were a key factor, particularly with shallower water depths over the intertidal mudflats.

1. Introduction

Microphytobenthos (MPB), the assemblages of autotrophic and heterotrophic algae, bacteria, fungi and protists and associated extracellular biofilm matrices, occur widely in intertidal and shallow subtidal soft sediment habitats (Underwood and Kromkamp 1999). In many estuarine systems, with shallow and turbid overlying water columns, MPB are the main primary producers, photosynthesising during periods of tidal emersion (Underwood et al., 2005; Hanlon et al., 2006). MPB can cover extensive areas of intertidal flats and show a range of seasonal and spatial patterns of distribution. Sunlight, wind, temperature, nutrients and grazing are important drivers regulating the biomass and productivity of MPB (Blanchard et al., 2001; Orvain et al., 2004;

Blanchard et al., 2006; Savelli et al., 2018; Rakotomalala et al., 2019). These drivers also correlate with the spatial patterns of biomass, productivity and species composition found across the intertidal gradient from upper to lower shore, and with different sediment particle sizes (Underwood 1994; Ribiero et al., 2013; Forster et al., 2006; Plante et al., 2016; Hill Spanik et al., 2019) and along estuarine salinity and nutrient gradients (Underwood and Paterson 1993; Forster et al., 2006; van der Wal et al., 2010). A key feature of MPB distribution is a high level of microspatial and micro-temporal variability in biomass (Spilmont et al., 2011; Weerman et al., 2011; Taylor et al., 2013; Daggers et al., 2020; Hope et al., 2020) underlying longer term seasonal and inter-annual patterns of variability (De Jonge et al., 2012; van der Wal et al., 2010; Benyoucef et al., 2014; Nedwell et al., 2016; Daggers et al., 2020).

Living on soft intertidal sediments, MPB assemblages are susceptible to physical disturbance from wind, rain, waves and tidal currents. Though MPB biofilms can stabilise sediments, increasing the critical shear stress needed to initiative erosion (Paterson 1989; Ubertini et al., 2015; Hope et al., 2020) through the production of extracellular polymeric substances (EPS), significant quantities of MPB can still be resuspended during tidal cover (Hanlon et al., 2006; Bellinger et al., 2009; Taylor et al., 2013; Savelli et al., 2019). In a key study, De Jonge and Van Beusekom (1995) determined that wind-induced waves and current velocities were responsible for resuspension of MPB in the Ems-Dollard estuary, with up to 50% of the phytoplankton Chl. *a* present in the water column originating from the mudflats. De Jonge and Van Beusekom (1995) also proposed that the effective wind speed threshold to allow MPB resuspension to happen varied spatially and temporally. Ubertini et al. (2012) also found significant temporal variability in levels of MPB resuspension in the Bays des Veys estuary in France. Rainfall during periods of tidal emersion disrupts biostabilisation of the sediment surface by EPS on muddy sediments, increasing sediment erodibility and losses of sediment Chl. *a* during tidal immersion (Tolhurst et al. 2006, 2008; Ha et al., 2018). Tidal currents and range may also play a role; sampling at 'within day' temporal scales found significantly higher suspended Chl *a* during spring than neap tide periods (Koh et al., 2006) with tidal range and currents important for lateral movements of suspended material between channels and mudflats (De Jonge and Van Beusekom 1995).

The ecological importance of MPB resuspension is reflected by the fact that MPB Chl. *a* appears to be the main contributor to water column primary production in some estuaries (Brito et al., 2012; Koh et al., 2006; Ubertini et al., 2012). Because MPB resuspension displays strong temporal and spatial variability, similar to the typical patterns of MPB biomass on sediment surfaces, resuspension events may be a key factor that controls the MPB biomass dynamics on an intertidal flat (Savelli et al., 2019).

In this study, we carried out a series of investigations to determine the importance of wind, waves, tidal range, sun and rain conditions on the spatial and temporal distribution of biofilm biomass (Chl. *a* and EPS), quantifying the exchanges of sediment and associated MPB from the mudflat surface into the water column over neap and spring tidal cycles during three periods of a year at a single site, typical of mudflats found within the Colne Estuary, U.K.. We measured sediment Chl. *a* and EPS concentrations, suspended solids and water column Chl. *a* and settling rates in the water column, and also used benthic diatom species composition to determine if the suspended Chl. *a* sediment-associated in the water column originated from biofilms on the adjacent sediment surface. By focusing on a single site, we minimized the confounding effects of macro-scale spatial variability, and the changes in sediment properties and nutrient conditions that occur along estuarine gradients (Underwood et al., 1998; Nedwell et al., 2016).

We hypothesized (1) that MPB resuspension (suspended Chl. *a* concentrations and species composition) would be positively related to measures of wind and wave energy (De Jonge and Van Beusekom, 1995), while wet weather would reduce the biostabilisation potential of MPB biofilms (Underwood, 1994; Tolhurst et al., 2003). We hypothesized (2) that the positive effect of bad weather on MPB resuspension will be greater during periods of increased tidal range, because higher water current energies with higher tidal ranges (as in spring tide) would resuspend more sediment and MPB, than the lower energy water currents during decreased tidal range (as in neap tide) (Koh et al., 2006). Conversely, periods of good weather and sunshine would increase sediment stability, and reduce resuspension events. Finally the aim was 3) to determine the relative importance of sediment settlement or deposition (Facca et al., 2002) with the availability of MPB biomass after immersion events within the matrix of weather-related abiotic factors.

2. Materials and methods

2.1. Sampling design and methods

Field sampling took place over 12–15 day periods during the months of April, July and October 2013, at the Fingringhoe tidal mudflat in the Colne estuary, Essex, U.K. (Fig. 1A). The study location comprised a mudflat approximately 13 ha in area, fringed with salt marsh, within the polyhaline section of the estuary (salinity ranging from 18 to 30, depending on freshwater flow conditions, Nedwell et al. (2016)). The Colne estuary is macro tidal (tidal range 5 m), with high turbidity inhibiting phytoplankton activity (Nedwell et al., 2016), and has high nitrogen and phosphorus loadings (McMellor and Underwood 2014). Sediment at the site was predominantly silts and clays (mean particle size 11.35 ± 1 SE μm) with particles < 63 μm contributing $92.24\% \pm 0.3$ SE of the total sediment, with a 5% proportion of 'very fine sand' particles >63 μm and <125 μm (Wood et al., 2015a). Mean surface sediment water content at the site was $62.3\% \pm 0.4$ SE (Maunder and Paterson, 2015). During summer 2013, the main macrofauna species present were the mud snail *Peringia ulvae* (average density of 194.8 ± 82 SE individuals m^{-2}; highest density 5093 m^{-2}), and low densities of *Hediste diversicolor* (7.7 ± 61 SE indiv m^{-2}) (Wood et al., 2015b). Transects consisting of eight 0.5 m × 0.5 m (Fig. 1B) quadrats with a spatial distances 5 m between quadrats, were laid out on the un-vegetated area of tidal flat parallel to the edge of the salt marsh (Fig. 1C), in two different zones; the transition zone below the salt marsh cliff (+1.19 m above U.K Ordnance datum (OD)) 5 m from the marsh cliff edge, and on the mudflat, 10 m further out from the transition zone transect (sediment height 1.10 OD). Both zones were below the mean high water neap tide level (+1.78 m above OD), so that the sediments were covered with water in every high tide through the whole tidal cycle.

Within each month, seven days of sampling (2 days during neap tides, 3 days in the following spring tide and 2 days in the later neap tide) were conducted over the neap-spring-neap tidal cycle (Table 1). On each sampling day, triplicate minicores (diameter 2.84 cm^2, top 2 mm of sediment surface) were taken randomly within each quadrat on the mud flat (3 × 8) and the transition zone (3 × 8). Samples were taken within the first 2 h after tidal emersion. Each top 2 mm sediment sample was divided into half; the first half was frozen and freeze-dried for Chl *a* and extracellular polymeric substance (EPS) analyses. Chl. *a* and EPS concentrations (μg cm^{-2}) were carried out according to Hanlon et al. (2006) and Lorenzen (1997). The second half of each minicore sample were analyzed for cells counts of diatom composition.

In conjunction with sediment sampling, sediment traps (inverted 850 mL capped plastic bottles with the top removed) were deployed on the mudflat to sample suspended sediment loading. Sediment trap sampling was done three times each month, during the early neap tide, (ENT), spring tide (ST) and later neap tide (LNT) periods. On the first sampling day of ENT, ST and LNT, two traps were attached vertically to canes marking the corners of each quadrat. One of the two deployed sediment traps on each quadrat was an empty 850 ml bottle which, after filling during tidal cover, determined the suspended solid load (mg L^{-1}). The second trap was an identical-designed bottle pre-filled with 2.3% NaCl (the salinity of the estuarine water at the site). Sediment collecting in this "filled" bottled was deemed to reflect the net vertical sediment settlement rate (mg cm^{-2} $hour^{-1}$) through the water column into the bottle during the period of tidal cover when the bottles were submerged. Sediment traps were collected and all contents transferred into 500 ml bottles on the following day. To determine Chl. *a* concentrations, samples were fully mixed and 250 ml of the sample was filtered using pre-weighed (after drying at 80 °C for 24 h) 12 cm diameter GF/F Whatman filter paper. Filters were freeze dried and weighed to determine sediment load (mg L^{-1}). Chl. *a* concentrations from the filter papers were then determined using the same methods as for sediments. In this study, Chl. *a* data from sediment sampled before the high tide in which
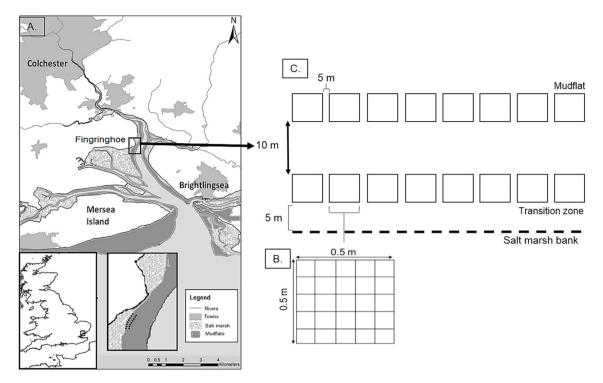
Fig. 1. Location of the A) sampling site at Fingringhoe Wick in the Colne Estuary, Essex, U.K.; B) the 0.5 × 0.5 m quadrats were laid out parallel to the shoreline on the C) transect, with 5 m distance between each other on the transition zone and on the mudflat.

Table 1
Variability of weather-related abiotic factors and tidal range across seven sampling days spanning neap and spring tide periods across three different sampling months, April 2013, July 2013 and October 2013. Mean wind speed (MWS) is the mean value of wind speed (m s^{-1}) on the sampling day + two days prior to the actual sampling occasion. Sum of rainfall (SOR) is the accumulative rainfall (mm) on the sampling day + two days prior to sampling day. Sum of sun hours (SOS) is the accumulative period of sun (hours) of the sampling day + two days before the sampling day. The data in bold indicate spring tide periods.

MONTH	WEATHER-RELATED FACTORS	SAMPLING DATE							SAMPLING MONTH
		4/4/13	5/4/13	9/4/13	10/4/13	11/4/13	17/4/13	18/4/13	APRIL 2013
Apr-13	MWS (m s^{-1})	14.5	8.1	**6.1**	**7.7**	**9.3**	2.4	17.4	8.2 ± 0.4
	SOS (hours)	11.8	13.8	**10.9**	**7.4**	**7.4**	8.6	12.4	9.3 ± 0.2
	SOR (mm)	1.4	1.4	**0.0**	**0.3**	**4.4**	2.4	1.0	0.6 ± 0.05
	TIDAL RANGE (m)	3.7	3.6	**4.3**	**4.6**	**4.8**	3.6	3.8	3.9 ± 0.0
		2/7/13	3/7/13	10/7/13	11/7/13	12/7/13	16/7/13	17/7/13	JULY 2013
Jul-13	MWS (m s^{-1})	2.8	4	**6.05**	**3.75**	**6.03**	3.6	1.9	3.4 ± 0.03
	SOS (hours)	21.4	8.3	**36.3**	**30.9**	**19.1**	20.5	24.9	24.2 ± 0.4
	SOR (mm)	0.0	3.7	**0.0**	**0.0**	**0.0**	0.0	0.0	0.0
	TIDAL RANGE (m)	3.9	4.1	**5.1**	**5.4**	**5.6**	3.9	4.2	4.4 ± 0.1
		2/10/13	3/10/13	8/10/13	9/10/13	10/10/13	15/10/13	16/10/13	OCT 2013
Oct-13	MWS (m s^{-1})	3.2	4.0	**3.2**	**4.8**	**9.3**	5.4	4.0	4.5 ± 0.1
	SOS (hours)	10.9	7.0	**17.1**	**10.3**	**12.3**	2.8	1.7	8 ± 0.3
	SOR (mm)	0.3	8.1	**0.6**	**0.6**	**5.4**	18.7	5.8	6.5 ± 0.7
	TIDAL RANGE (m)	3.7	4.0	**4.6**	**4.8**	**5.1**	3.9	4.0	4.1 ± 0.0

sediment trap samples were collected were used to investigate sediment-water column exchanges of sediment and Chl. *a*.

Diatom cells were cleaned following an acid washing procedure to generate cleaned diatom frustules (Underwood, 1994). For each mini-core sample, a permanent slide of cleaned frustules was made using half of the sample. A total of 400 valves were identified and counted for each surface sediment sample for both the mud flat and the transition zone in the April and July 2013 samples. However, only 250 valves per samples were counted in the October 2013 samples due to low cells densities. A total of 200 ml water sample from sediment traps were centrifuged (1500 rpm for 10 min) to separate the sediment and associated diatoms from water. The supernatant was discarded (150 ml) using soft plastic tubing, while the remaining 50 ml sample was agitated, collected and transferred into 50 ml tube. The collected sample was then centrifuged at 2300 rpm for 15 min. For fresh samples, 5 ml of the centrifuged

sample was transferred into bijou bottle and was preserved in 0.5% glutaraldehyde in 2.3 saline (NaCl) water. The remaining sample was used in acid washing procedure (Underwood, 1994) for permanent slide preparation with a total of 200 diatom valves counted for assemblage composition analysis.

Data for weather-related abiotic factors; i.e., daily rainfall, the number of sun hours (hours each day of direct sunlight, not occluded by cloud) were obtained from Colchester Weather Site based in the Myland, Colchester, Essex, UK (http://www.tijou.co.uk/weather/). The weather site is the nearest weather site from the sampling site (at the distance of 6.1 km). Data for wind speed and wave height at the Fingringhoe tidal flat were provided courtesy of Professor Tom Spencer and Dr Ben Evans of the University of Cambridge, using wave monitoring equipment that was installed at Fingringhoe tidal flat. Daily tidal variation were obtained from www.TideTimes.org.uk for Brightlingsea. Rainfall data was

calculated as the 'sum of rainfall' (mm) of the two days before sampling days and on the sampling day up to the period of sampling. A similar 3 day period was used to calculate the 'sum of sun hours' (hour). The average wind speed data for three days (two days before sampling day + on sampling day) was calculated and reported as the 'mean wind speed' (m s^{-1}) (De Jonge et al., 1995; Booth et al., 2000). The mean values were used after taking into account the data analyses result from our pilot data, which showed MPB biomass correlated more significantly with averaged data (mean) rather than the non-averaged data.

2.2. Statistical analysis

Combined Chl. *a* (n = 504) and EPS (n = 504) data for the whole study were analyzed using general linear model (GLM) in Minitab 19.0 statistical software packages. This GLM was done to investigate the percentage of contribution of each factor to the variability of the Chl. a and EPS (Fig. 3). The analyses were done separately for each zone. The months, sampling days within months and spatial scale <5 m (between quadrats) nested in months and days factors, were computed as the factor, while the logged transformed of both Chl. *a* and EPS were the responses (done separately).

To investigate the MPB sediment-water column exchanges at our study site, the Chl. *a* and EPS data on the sediment surface were compared with the suspended sediment, suspended Chl *a* and the settlement rate data. Beforehand, the variability of the mentioned variables between zones (n = 2, d.f. = 1), between months nested within zones (n = 6, d.f. = 4) and between days within month nested in zones (n = 42, d. f. = 36) were analyzed by means of the GLM analyses in Minitab 19.0 (n = 1008, for benthic Chl. *a* and EPS only). Post hoc Tukey Tests (using Minitab Statistical Software 19.0) were carried out to reveal the variability of Chl. *a* and EPS within factors. Use of data comparison between benthic and suspended and between benthic and deposited (settlement) properties were detailed in Table A1, Appendix A.

To analyze the Chl. *a* and EPS variability between tidal types, only the data from sampling on the day when the sediment traps were deployed (transformed log$_{10}$), were used. The factor tidal type were classed as three levels, the early neap tide, spring tide and later neap tide) (n = 72 for each zone for each level). This grouping were done to eliminate the unequal variances due to unbalanced sample size between spring (n = 144 for each variable) and neap tides (n = 288 for each variable). Tukey Pairwise post hoc comparisons were performed on the data. Groups that do not share similar letters indicates statistically significant differences in means (Table A2 Appendix A). Pearson correlation coefficients were used to investigate for any relationship analyses. Beforehand, all the analyzed data were transformed by means of log$_{10}$ transformation.

Multiple regression was used to model the relationship between the SS and SS$_{Chl. a}$ and the mentioned chosen abiotic factors. The analyses were carried out separately according to zones. Using Minitab 19.0 software (Minitab, 2020), in each analyses, SS and SS$_{Chl a}$ was set as the response, whereas the MWS, SOR, SOS and tidal range were set as predictors. Beforehand, the predictors were initially checked for multicolinearity. Stepwise method was chosen to run the analyses, in which the predictors for which *p* value greater than α = 0.05 were removed from the model.

Principal component analyses were performed using FactoMineR (Lê et al., 2008) in R stat. The analyses were done on the log transformed of suspended variables (suspended sediment and suspended Chl *a*) and sediment surface variables (Chl *a* and EPS) of pooled mud flat and transition zone data. The individual scores of the PCA were analyzed to identify for temporal trends. Only the first and the second component of the PCA were retained and used in the results and discussion.

Four hundred and thirty two diatom samples were counted (with 400 values identified per slide for benthic samples and 200 valves for sediment trap samples), and the diatoms identified using standard texts (Witkowski et al., 2000). Counts for each species were expressed as

relative abundance, and triplicate samples from each sediment quadrat were averaged to create a community composition profile for that quadrat. Sediment trap data and benthic data (from mudflat and from transition zone) were compared, with the trap data compared to the sediment assemblage sampled on the low tide before trap deployment. Diatom assemblage composition analyses (NMDS, ANOSIM and SIMPER) were conducted on the diatom species-abundance Bray Curtis dissimilarity matrix using R version 4.0 with the package vegan (R Core Team, 2020; Oksanen et al., 2019).

Modified Morisita Similarity Index was performed to investigate the similarity between the MPB species composition on the sediment surface and in the water column (in the trap). The Multi Variate Statistical Package (MVSP) 3.1 software (Kovach, 1999) was used to carry out the mentioned similarity index analyses. Scores of Morisita index that ranges from 0 (no similarity) to 1 (complete similarity) were converted into percentage values to further investigate the similarity of the two mentioned variables.

3. Results

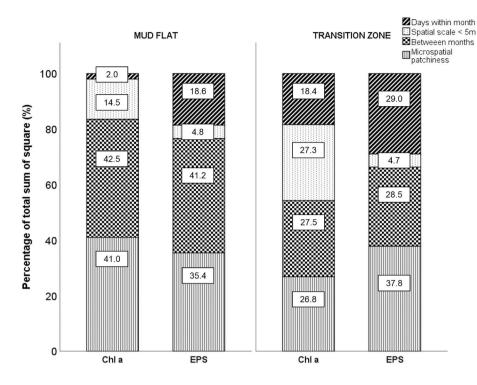### 3.1. Variability in benthic Chl a and EPS concentrations across an intertidal flat

Average sediment Chl. *a* concentrations on both zones ranged between 4.4 and 13.2 µg cm^{-2} over the three periods of sampling (Fig. 3A), with no consistent pattern of significant differences between the mud flat and the transition zone. In both the mudflat and transition zone, Chl. *a* concentration in both zones showed significant variation between sampling months ($p < 0.01$). Only Chl. *a* concentration on the transition zone significantly varied between dates nested in month ($p < 0.001$). Based on the calculated percentage of sum of squares (SOS), the greatest contributions to variability in biomass (Chl. *a* and EPS) were the microspatial and spatial scales (at distances of <0.5 m and <5 m respectively), and between months (Fig. 2).

In contrast to average sediment Chl. *a*, the average EPS concentration was relatively higher on the mud flat compared to the transition zone sediments (Fig. 1B). There was a high level of daily temporal variability in sediment EPS concentrations, with significant differences between sampling months, sampling dates and between quadrats (spatial < 5 m) (all at $p < 0.001$) (Fig. 3B). Based on the calculated percentage of sum of squares (SOS), more than 18% of the EPS variability was due to variability between sampling days (Fig. 2). Concentration of EPS on the sediment surface also exhibited variation even between replicates, at micro-spatial level, similar to that seen for sediment Chl. *a* (Fig. 2).

Chl. *a* concentration between the three tidal periods (EN, SP, LN) on both zones displayed similar patterns with no significant differences (Table A2, Appendix A). Contrarily on the mud flat, the EPS concentration on the transition zone was varied significantly between tidal periods ($F_{2,207} = 28.66$, $p < 0.001$). Tukey Pairwise comparisons output supported the significant difference in benthic EPS concentration between the tides, with the highest mean recorded during spring tide (162.7 ± 14.2 µg gluc. equiv. cm^{-2}) (Table A2, Appendix A) (Fig. 3B).

Over the different periods of study, average high tide suspended sediment concentration (SS) varied between 184 and 1825 mg L^{-1} (Fig. 3C). Both SS and suspended Chl *a* (SS$_{Chl a}$) concentrations were significantly higher in water over the transition zone (SS: 1187.7 ± 53.4 mg L^{-1}; SS$_{Chl a}$: 109.6 ± 7.15 µg Chl. *a* L^{-1})) than in water sampled over the mud flat (SS: 934.5 ± 55.8 mg L^{-1}; SS$_{Chl a}$: 89.13 ± 7.57 µg Chl. *a* L^{-1}) (SS ($F_{1,381} = 11.39$, $p < 0.001$); SS$_{Chl a}$ ($F_{1,381} = 61.5$, $p < 0.001$)) (Fig. 3C and D, respectively) (Fig. 3C and D). There were significant differences in SS and SS$_{Chl a}$ between days nested in month of each zone ($F_{14,381} = 27.1$, $p < 0.001$ and $F_{14,381} = 38.6$, $p < 0.001$, respectively). Only SS$_{Chl a}$ was significantly varied between months ($p < 0.001$).There was significantly higher SS and SS$_{Chl a}$ on both the mudflat and transition zone during early and later neap than in spring tide at $p < 0.01$.

There were significant positive correlations between water column

Fig. 2. Percent partitioning of variability (total sum of squares from Nested General Linear Model) between sampling months (n = 3, degrees of freedom (d.f.) = 2), days nested in months (n = 21, d.f. = 18), between spatial scale < 5 m nested in days and months (n = 168, d.f. = 147) and between replicates (microspatial patchiness/error) of Chl a and EPS concentrations in top 2 mm (μg cm^{-2}) sediment of the mud flat and of the transition zone of Fingringhoe tidal flat, Colne estuary, U.K. Microspatial patchiness is the lowest scale (between triplicate samples within a quadrat) which represents the individual minicores within quadrats. The samples size for each of the dependent variables is n = 504.

suspended sediment load (SS) and water column Chl. a concentrations (SS$_{Chl\ a}$) (Pearson correlation coefficients for overall data, r = 0.561, $p <$ 0.001) in all three sampling months (Fig. 4). However, the gradients of the linear relationship between SS$_{Chl\ a}$ and SS differed significantly between the three seasons, and between the transition and mud flat zones. The steepest gradients occurred in April and July on both the mud flat (Fig. 4A) and the transition zone (Fig. 4B). The weakest correlation between SS and SS$_{Chl\ a}$ (explaining 20.9% of the variability) was on the transition zone in April 2013, where the relationship only (Fig. 4B). Low SS$_{Chl\ a}$ during October 2013 was concurrent with the month's low sediment Chl. a (Fig. 3A and C). There was a significant relationship between the gradient of the slope for each month with the monthly average concentration of Chl. a on the sediment surface (Pearson correlation of r = 0.768, $p < 0.05$). The significant relationship confirmed that the positive relationship between SS$_{Chl\ a}$ and SS was closely related to the availability of Chl. a on the sediment surface.

3.2. Relationship between suspended sediment load and suspended Chl. a concentrations and abiotic physical factors

Mean wind speed varied over the three monthly periods (Table 1). April 2013 was the windiest month with the mean wind velocity significantly higher than in July and October 2013 (both significant at $p < 0.001$) (Table 1). July 2013 (summer) had the lowest mean wind speeds. At the Fingringhoe site, wind speed was significantly positively correlated (r = 0.648, $p < 0.001$) to wave height over the tidal flat (Appendix A Figure A1). Sum of rainfall varied significantly between sampling months ($p < 0.001$) (Table 1), with October the wettest period, and July 2013 the driest. Both April and July received significantly lower ($p < 0.001$) rain than October 2013. The driest month (July 2013) had the longest period of sun hours, significantly higher than April ($p < 0.001$) and October 2013 ($p < 0.001$) (Table 1).

Levels of wind and rainfall on the days prior to sampling, and tidal range, had significant effects on SS$_{Chl\ a}$ over the mudflat, with the slope gradient of the relationship between SS$_{Chl\ a}$ and SS significantly positively correlated with mean wind speed (r = 0.644, $p < 0.001$), and significantly negatively correlated with tidal range (r = −0.396, $p <$ 0.001) and the sum of rainfall (r = −0.239, $p < 0.05$). These
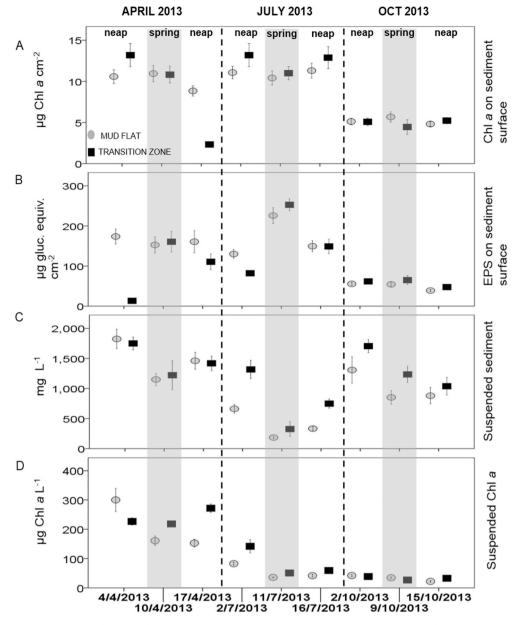
relationships with weather-related physical factors were weaker over the transition zone, where the gradient of SS$_{Chl\ a}$ and SS was only significant correlated (negative) with the sum of rainfall (r = −0.339, p < 0.01). The sum of sun hours on both zones showed no significant correlations with the gradient of SS$_{Chl\ a}$ and SS.

Multiple regression analyses established that all of the four weather-related abiotic factors significantly predicted the SS and SS$_{Chl\ a}$ on both zones (Table 2A & 2B). Wind speed was a significant positive predictor of SS and SS$_{Chl\ a}$, with the stronger effect on the mud flat than on transition (Table 2). The sum of sun hours was the strongest predictor of SS on both zones. An increase of 1 h to the sun hour significantly predicted the decreased of 41.3 and 31.5 mg L^{-1} of SS on the mud flat and the transition, respectively. Sun hours however was not a significant predictor of SS$_{Chl\ a}$ on both zones. (Table 2B). Larger tidal range tides on the transition zone had stronger negative effect on both SS and SS$_{Chl\ a}$ than on the mud flat. SS on the mud flat was the least affected by tidal range, significantly predicted only at $p < 0.05$. Increased rainfall significantly predicted the increase in SS, but a decrease in SS$_{Chl\ a}$ on both zones (Table 2A & 2B). An increase in 1 mm of rainfall was predicted to increase sediment resuspension in the water column to more than 30 mg L^{-1}, but reduces more than 5 μg of Chl. a per L of water.

3.3. Determining the relationship between benthic biomass, suspended biomass and weather-related variables

Principal Components Analysis (PCA) was carried out to determine the relationship between benthic and suspended microalgal biomass and weather-related abiotic variables. Principal Components 1 and 2 from PCA of the log-transformed of the water column variables (SS and SS$_{Chl\ a}$) and sediment surface variables (Chl a and EPS concentration) for the pooled mud flat and transition zone data explained 76.05% of the total variation (Fig. 5).

Principle component 1 (PC 1) represented a gradient positively correlated with SS$_{Chl\ a}$ and SS and negatively correlated with microphytobenthic biomass-related measures (sediment Chl a and EPS concentrations) (Fig. 5, Table 3). PC 1 scores of individual samples were also independently positively correlated with increasing mean wind speed (r = 0.251, $p < 0.001$) (Table 2). PC1 scores for both April and October

Fig. 3. Temporal variability (mean ± SE, all n = 8 unless mentioned) of A) surface sediment Chl. *a* concentrations; B) sediment EPS concentrations; C) suspended sediment load; D) water column suspended Chl *a* concentration on the Fingringhoe tidal flat in Colne estuary, U.K., in April, July and October 2013.
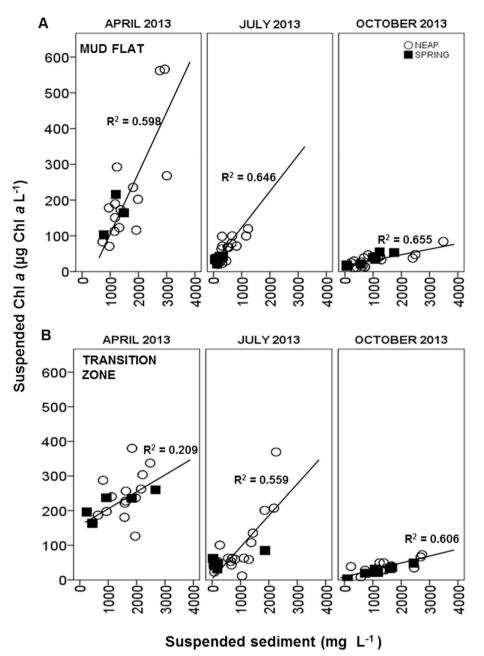
2013 were more positive on PC1 than July 2013, and characterized by higher SS and high SS$_{Chl\,a}$ (only for April 2013), and higher mean wind speed (Table 1). PC 1 scores were significantly negatively correlated with tidal range (r = −0.423, p < 0.001) (Table 3), corresponding to significantly higher average SS (1193 ± 46 mg L^{-1}) and average SS$_{Chl\,a}$ (114 ± 7 µg Chl. *a* L^{-1}) during neap than in spring tide (Fig. 3C & D).

Principal component 2 (PC 2) explained 32.24% of total variation (Fig. 5), and was positively correlated with microphytobenthic biomass indicators (Chl. *a* and EPS concentrations), and increased water column SS and SS$_{Chl\,a}$ (Table 3). Positive sample scores on PC 2 indicated that SS$_{Chl\,a}$ in the water column was positively related to the availability of the Chl *a* on the sediment surface, and to higher wind speeds (r = 0.393, p < 0.001) (Table 3). Samples from October 2013, that had significantly lower PC 2 scores than the other two months (p < 0.001), were characterized by significantly lower Chl. *a* and EPS concentrations than in April 2013 and July 2013 (Fig. 3A and B and 5). There were significantly lower Chl. *a* concentrations on the sediment surface in October 2013 than in April and July 2013 (both significant at p < 0.001),

corresponding to low SS$_{Chl\,a}$ in October 2013. 'Sum of rainfall for three days' was significantly negatively correlated with PC 2 sample scores (r = - 0.361, p < 0.001) (Table 3). Significantly higher rainfall in October 2013 (Table 1) may be responsible for the low biomass concentration recorded on the sediment surface and also the low suspended Chl *a* recorded in the water column (Fig. 4).

3.4. Transfer of MPB species between the sediment surface and the water column

Sixty five diatom taxa were identified in the surface sediment samples across the study site (Table A3). Of these, thirty-four species were also identified in the sediment trap samples of either mud flat or transition zone or both zones (Table A3). Common taxa, present in high relative abundance in both the mudflat and transition zone benthic assemblages include *Gyrosigma balticum*, *G. scalproides*, *G. limonsum*, *Pleurosigma angulatum*, *Nitzschia sigma*, *Nitzschia panduriformis* and *Navicula gregaria*. There were significant differences in assemblage

Fig. 4. Relationships between suspended sediment (SS) and suspended Chl a (SS$_{Chl\ a}$) across the neap-spring tidal cycle on; A) the mud flat and; B) the transition zone, in April 2013, July 2013 and October 2013. R^2 values from linear regression between SS$_{Chl\ a}$ and SS, n = 8.

composition between the mudflat and transition zone (Fig. A3, Appendix A), ANOSIM, r = 0.506, $p < 0.001$), caused by higher RA of *Nitzschia dubia*, *Nz navicularis*, and *Nz. punctata*, and also a number of planktonic taxa, *Coscinodiscus*, *Stephanodiscus*, *Odontella aurita* and *Actinoptychus splendens* on the MF (SIMPER, $p < 0.001$ in all cases) and higher RA of the large pennate diatoms *G. wansbeckii*, *Scolioneis tumida*, *Stauroneis producta*, *Cymatopleura solea*, *Plagiotropis vitrea*, *Diploneis didyma* and *Berkeleya scopulorum* on the transition zone (SIMPER, $p < 0.001$ in all cases). Within each month, assemblages were similar between quadrats, with some shifts over the tidal cycle, with a tendency to slightly higher RA of planktonic centric diatoms during Spring tide days. However, overall, tidal stage did not significantly alter the overall benthic diatom assemblage composition. There was a significant shift in the composition of both the mudflat and transition zone assemblages between months, and particularly in October (Figure A3, ANOSIM, r = 0.451, p < 0.001), with significantly increased RA of *Raphoneis minutissima*,

Nitzschia acuminata, *Navicula gregaria*, *N. deurrebergiana*, *Fallacia forcipata* and *Tryblionella* sp. (SIMPER, $p < 0.001$) on mudflat and transition zone sites during October.

There were significant differences in the composition of the diatom assemblages between the benthic and sediment trap sampled in the three different months (Fig. 6). The major separation was attributable to differences between sediment versus water column, and mudflat versus transition zones (ANOSIM, R = 0.514, $p < 0.001$). The commonest taxa found in sediment traps were predominantly benthic pennate diatom species, with increased RA of *G. wandbeckii*, *G. fasciola*, *N. gregaria*, *Calonies formosa*, *S. tumida*, (SIMPER, $p < 0.05$) in mudflat sediment traps compared to benthic mudflat assemblages, but also increased RA of the centric diatoms *Actinoptychus splendens*, *A. undulatus*, *Coscinodsicus* sp3, *Odontella aurita* and *Stephanodiscus* sp1 (SIMPER, $p < 0.05$), particular in Spring tide samples (Table A3). Transition zone sediment traps showed increased RA of *D. didyma*, *Triceratium* (SIMPER $p < 0.01$),

Table 2
Multiple regression outputs between A) SS and B) SSChl a and weather-related abiotic factors and tidal range for the mudflat and transition zones at Fringringhoe, Colne estuary.

	Mudflat			Transition		
A) Suspended sediment						
Regression	$R^2 = 35.6\%$, $F_{4, 197} = 26.69$, $p < 0.001$			$R^2 = 45\%$, $F_{3, 200} = 27.3$, $p < 0.001$		
	Coefficient	F value	*p* value	Coefficient	F value	*p* value
Predictor						
Mean wind speed	58.5	19.4	***	26.2	4.0	*
Sum of sun	−41.3	28.3	***	−31.5	16.9	***
Sum of rainfall	37.6	17.2	***	36.7	15.9	***
Tidal range	−231.5	6.4	*	−333.0	13.5	***
B) Suspended Chl. *a*						
Regression	$R^2 = 52.0\%$, $F_{3, 197} = 70.1$, $p < 0.001$			$R^2 = 33.1\%$, $F_{3, 200} = 32.5$, $p < 0.001$		
	Coefficient	F value	*p* value	Coefficient	F value	*p* value
Predictor						
Mean wind speed	18.7	149.4	***	9.9	36.6	***
Sum of sun	**Ns**	Ns	ns	ns	ns	ns
Sum of rainfall	−5.4	36.1	***	−5.9	34.3	***
Tidal range	−49.7	30.0	***	−56.6	30.1	***

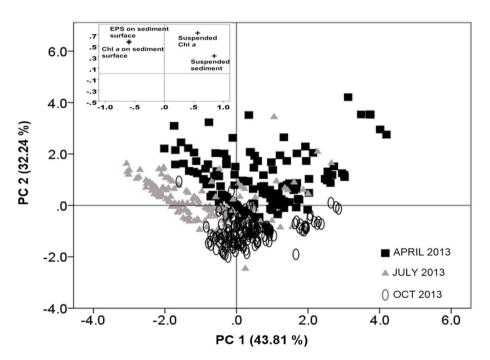*** Significant at $p < 0.001$.
** Significant at $p < 0.01$.
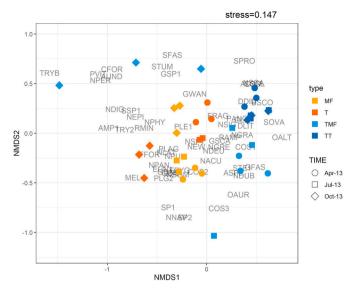*Significant at $p < 0.05$.
ns is not significant.

Fig. 5. Scatter plot of components 1 and 2 from principal component analysis (PCA) of log-transformed data (mud flat and transition zone individual measurements) of Chl. *a* and EPS on the sediment surface and suspended properties (SS and $SS_{Chl\ a}$) across three sampling months coded by sampling months; April 2013, July 2013 and October 2013. Inset graph show the locations within the PC1 – PC2 space of the measured factors in the PCA analyses.

Table 3
Pearson's correlation coefficients (r) between principle component 1 (PC 1) and 2 (PC 2) with Chl *a* and EPS concentrations on the sediment surface, and with the measured weather-related abiotic factors; the mean wind speed (m s^{-1}), sum of rainfall (mm), sum of sun hours (hour), and tidal range (m). *** indicates significant different at $p < 0.001$, ** indicates significant different at $p < 0.01$ and * indicates significant different at $p < 0.05$.

Principle component (PC)	Biological factors		Sediment		Weather-related abiotic factors			
	Chl *a* (on sediment surface)	EPS (on sediment surface)	SS	$SS_{Chl\ a}$	Mean wind speed	Sum of rainfall	Sum of sun	Tidal range
PC 1	−0.599***	−0.604***	0.845***	0.566***	0.251***	ns	−0.505***	−0.423***
PC 2	0.583***	0.565***	0.582***	0.732***	0.393***	−0.361***	0.174***	ns

Fig. 6. NMDS plot of species composition of benthic diatom assemblages (relative abundance) sampled from mudflat (M) and transition (T) zone sediments and in corresponding sediment traps (TMF, TT) at Fingringhoe, Colne Estuary, Essex, U.K., during three sampling events (EN, SP, LN tides) in three different months in 2013. n = 8 replicate quadrats sampled each time. Labels indicate location of species scores in the NMDS space, see Table A2 for species names and codes).

and *P. angulatum, G limosum, B. scopolorum, Nz scalproides*, and *Surirella ova, C. solea, Achnanthes longipes* as well as *Coscindiscus* sp1 (SIMPER *p* < 0.01) compared with transition zone benthic assemblages (Fig. 6). Despite being abundant in the sediment, *G. balticum* was never recorded in the sediment traps on the transition zone (Table A3). Many of the centric taxa had higher relative abundances in the water column during spring tides (Table A3).

Comparison of the assemblage species composition revealed a positive correlation between the SS load and the % similarity between the diatom species composition on the sediment surface and in the water column, which explained more than 50% of the total variability across on both zones in April (R^2; 0.545) and July 2013 (R^2; 0.604) (Fig. 7). The relationship in October 2013 only explained 32.3% of the total variation. This close coupling of species similarity is evidence that the $SS_{Chl\ a}$ in the water column over the mudflat – transition zones originated from the sediments.

3.5. Sediment settlement and MPB biomass on sediment surface

The net sediment settlement rate was significantly positively correlated with benthic Chl. *a* (r = 0.211, *p* < 0.01) (Fig. A2). The significant variability in sediment settlement rate between the 3 months ($F_{2,398}$ = 38.155, *p* < 0.001) was related to the variability of the weather-related abiotic factors. Higher mean wind speeds (Table 1) were significantly negatively correlated with the net sediment settlement rate (r = - 0.359, *p* < 0.001 (Fig. 8 & Fig. A2, Appendix A). Relatively higher sediment settlement rates occurred during neap tide than in spring tide (Fig. A2), resulting in a significantly negative relationship between the sediment settlement rate and tidal range (r = −0.416, *p* < 0.001) (Fig. 8). The higher suspended sediment loads during neap tide compared to during spring tide indicates that the net sediment settlement rate is positively influenced by the sediment availability in the water column.

4. Discussion

A combination of high intensity sampling at a range of spatial and temporal scales, and parallel measures of benthic and water column suspended solid and suspended Chl. *a* concentrations, enabled a number of conclusions concerning key drivers influencing variability in MPB biomass and sediment-water column exchanges of MPB on tidal flats to be made.

4.1. Spatial and temporal variability in MPB biomass on sediment surface and in the water column

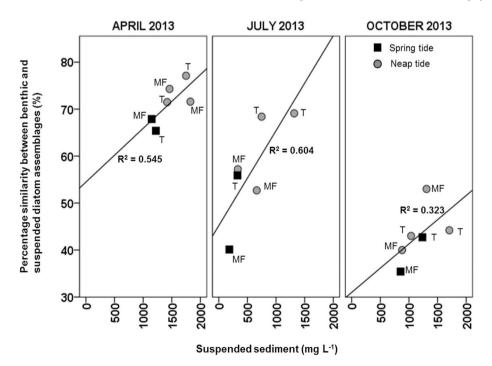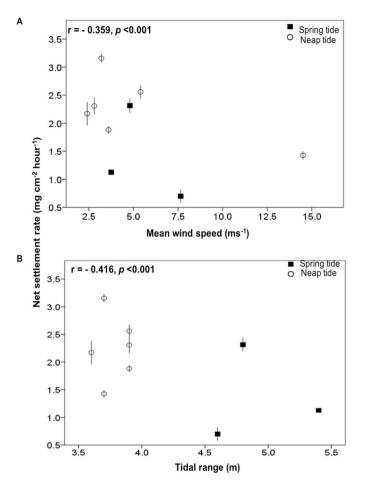The patterns of distribution of microphytobenthic biomass on

Fig. 7. Relationship between the suspended sediment load (SS) and the percentage similarity between the species composition of diatom assemblages on the sediment surface and the assemblage present in suspended sediment traps on the mud flat (MF) and the transition zone (T) in April, July and October 2013. The percentage similarity was determined by using the Modified Morisita similarity index test.

Fig. 8. Scatterplot between the net settlement of sediment with; A) mean wind speed for three days (Pearson Correlation Coefficient, $r = -0.359$, $p < 0.001$) and; B) tidal range across the neap-spring-neap tidal cycle. Values are mean ± SE, n = 16 (pooled data of the mud flat and the transition zone).

intertidal flats can be driven by spatial patchiness factors, and by temporal variability operating over scales from daily, within tidal phase, and monthly or seasonally (Nedwell et al., 2016). High levels of spatial patchiness are characteristic of MPB in intertidal mudflat and sandflat environments, with microspatial patchiness (<1 m scales between minicores) contributing between 36 and 60% of total variability (Spilmont et al., 2011; Weerman et al., 2011; Taylor et al., 2013). Some of this variability may reflect under-sampling at the meter scale (Spilmont et al., 2011; Tomas, 1997) but genuine patterns of patchiness, linked to small scale differences in topography, water content and biofilm presence, do occur (Weerman et al., 2011; 2012). Within each of the three periods of sampling, we took 336 minicore samples, nested within zone, quadrat, tide state and day. Spatial factors (microspatial within 0.5 m² quadrats, and at horizontal distances of 5 m), accounted for 26.7–41.0% and 4.7–27.3% respectively of the variability in the sediment Chl *a* concentration data, with greater microspatial variability on the mudflats, values in agreement with previous studies. Causes of these spatial patterns include patchy localized erosion of biofilms and regrowth (Hanlon et al., 2006; Weerman et al., 2012; Daggers et al., 2020), localized grazing pressure (particularly *Peringia ulvae*) (Austen et al., 1999; Orvain et al., 2004, 2006; Orvain et al., 2004a,b) and localized differences in sediment size and water content (Azovsky et al., 2004; Tolhurst et al., 2008; Launeau et al., 2018). Microspatial variability was unlikely to be caused by nutrient loadings or weather-related factors, as these apply equally across the spatial scales of an individual mudflat, and sediment composition is homogenous across this site (Wood et al., 2015a). Up to 18% of the total variability was accounted for by daily

differences in concentrations. Stochastic processes are important (Benyoucef et al., 2013), and the PCA showed that abiotic factors (weather and tide) also contributed to the varability in the sediment Chl a and sediment EPS concentrations.

Mudflat - salt marsh interfaces in temperate zones are often characterized by a transition zone; a mud cliff subject to lateral erosion and areas of eroded salt marsh blocks (Zhu et al., 2019). We did not find any significant differences in MPB biomass between the transition and mudflat zones, though the species composition was different. Patterns of biomass distribution across intertidal height gradients do occur, linked to periods of tidal exposure, water content and sediment stability (Underwood and Paterson 1993; Thornton et al., 2002; Forster et al., 2006; van der Wal et al., 2010; Orvain et al., 2012) with maximum biomass often found around midshore tidal height. However, in our study, the vertical height difference between the mudflat and transition zone sites was 10 cm, meaning that differences in the periods of tidal emersion would be only around 30 min per tide. High tide water over the transition zone at Fingringhoe was typified by higher suspended sediment and Chl. *a* concentrations than over the adjacent mud flat. Incoming tide water gathers organic and inorganic material as it travels across a mudflat, creating a turbid tidal edge with very high suspended solid load, that then decreases as water deepens and flow declines (Christie and Dyer, 1998). The transition zone also potentially received input of sediment and associated MPB from the eroded salt marsh bank during the immersion period (Mitchell et al., 2003). Saltmarsh MPB are deposited on the transition zone at Fringringhoe on ebbing Spring tides (Redzuan and Underwood, 2020), which may have contributed to the differences in assemblages.

Temporal variability in sediment microphytobenthic Chl. *a* concentrations accounted for between 2 and 43% of the variability measured, mainly present at the temporal scale between months (Fig. 2). Daily variability was low (less than 5% on the mudflats) but higher in the transition zone (18.4%). This range of monthly variability is in line with previous studies in the Colne estuary (Thornton et al., 2002), including a 23 year time series (Nedwell et al., 2016), and in other European estuary systems (van der Wal et al., 2010; Benyoucef et al., 2013). The seasonal patterns of grazer abundance also effect MPB biomass (Sahan et al., 2007). On the Fringringhoe flats, observations revealed high density of *Peringia* sp. on the sediment surface of the mud flat and the transition zone of the Fingringhoe tidal flat during all three sampling periods. *Peringia* sp. is one of the dominant sediment infauna of the Colne estuary (Chesman et al., 2006; Bellinger et al., 2009), and is a well-known deposit feeder that significantly affect the erodibility of MPB biofilms on intertidal flats (Hagerthey et al., 2002; Orvain et al., 2004, 2006). *Peringia* occurs in patches in the Colne and these aggregations of individuals move across the intertidal ((Bellinger et al., 2009; Booty et al., 2020), which may have contributed to spatial and temporal variability in MPB biomass. With respect that there was seasonal occurrence of *Peringia* sp. at the study site, it is potentially an important contributor to MPB biomass variability. Variability in *Peringia* densities, however, were not investigated in this present study.

4.2. How much MPB on the sediment reflects MPB in the water column

Resuspension and lateral transport of MPB biomass can be an important physical disturbance factor on intertidal mudflats. In the Ems-Dollard estuary (Netherlands), 20–25% of the Chl. *a* in the water column could be MPB, and this accounted for 14–25% of the total MPB biomass in the estuary, with a strong linear relationship between degree of MPB resuspension and windspeed (De Jonge and Van Beusekom, 1995). In our study, suspended solid loads (SS) and Chl *a* ($SS_{Chl\ a}$) concentrations were linearly related, with seasonal differences in the slopes and concentrations (Fig. 4). However, a strong correlation between the suspended sediment and suspended Chl *a* is not sufficient to prove that the suspended sediment and the associated Chl *a* originated from the local sediment surface.

The occurrence of sediment-water column exchanges across the mudflat was confirmed by diatom species composition data, with a strong positive relationship between the % similarity between the species composition of diatoms present in sediment traps and the benthic MPB assemblage, with increased suspended solid load. The majority of diatom species found in the sediment traps were pennate diatom taxa, also found in the sediments at the site, and characteristic of intertidal mudflats in the Colne (Underwood et al., 1998). Consistent differences in assemblage composition between the mudflat and transition were due to relative differences of taxa, not presence or absence of dominant species. This suggests that some distinct niche-driven factors (Plante et al., 2016) were operating to influencing relative abundance over this short distance. It is not possible to determine what these were, as the major known drivers of composition (nutrients, light, sediment type) were homogenous at a macro-scale across the site. The larger shift in assemblage composition (on both mudflat and transition) in October would indcate a strong seasonal or weather-related driver, with more tychoplanktonic taxa present (Underwood and Paterson 1993, Ribiero et al., 2013). Higher suspended sediment loads with an increased similarity in species composition to that of the sediment surface supported the idea that there were MPB sediment-water column exchanges across tidal flat. This conclusion is supported by the observation that there were corresponding changes in both the suspended and benthic diatom composition during the three different months of sampling, such that the percentage similarity relationships of the benthic biofilm were present each month. Similarity between benthic and water column diatom composition (71 out of 166 species recorded) was also seen at stations characterized by high sediment resuspension in the Venice lagoon (Facca et al., 2002).

Highest suspended solid concentrations were found during neap tide periods, with the highest diatom species assemblage similarities between benthic and water column, demonstrating the local origin of the sediments. Koh et al. (2006) also reported that MPB resuspension on tidal flat was affected by spring-neap tide variation. With the higher tidal ranges during Spring tides (an increased in high tide levels of approx. +1 m), suspended solid loads were lower across the site, and also contained many more planktonic centric diatom taxa (e.g. *Actinoptychus*, *Coscinodiscus*), thus lowering the overall % similarity. A number of these centric and small pennate taxa (e.g. *Odontella, Raphoneis, Cymatosira)* are tychoplanktonic, and found on both the sediment surface and with a higher abundance in the suspended water column. But the increased presence of centric phytoplankton taxa indicates a more coastal – offshore origin of the overlying water during spring tides (Brito et al., 2012). High tidal ranges during spring tides brings in planktonic centric diatom from adjacent water channels onto the tidal flats (Facca et al., 2002), some of which were deposited into the benthos, even though the net sediment settlement rate was low. Therefore, the species that were common during neap tides represent the local MPB community of the estuary. There was thus a greater degree of sediment remobilisation and deposition across the muflat – transition zone during neap tides than springs, despite the greater volumes of water moved within the estuary on spring tides.

Our data confirm the importance of hydrodynamics and weather conditions in determining the degree of the sediment-water column exchanges (De Jonge and Van Beusekom 1995; Koh et al., 2006; Ubertini et al., 2012). The temporal variability in sediment-water column exchange was most significant affected by mean three-day wind speed. There was a significant positive correlation between wind speed and wave height (r = 0.648, $p < 0.001$) (Figure A1, Appendix A), indicated the role of wind induced waves at out study site. Wind-induced waves generate sediment resuspension (French and Spencer, 1993; Booth et al., 2000) and MPB resuspension (De Jonge and Van Beusekom, 1995; Easley et al., 2005; Ubertini et al., 2015) on the mud flat and the transition zone during immersion periods.

High wind speed for 3 day at our study site significantly predicted the increased the SS and $SS_{Chl. a}$ in the water column, consistent with the

studies by De Jonge and Van Beusekom (1995) and Koh et al. (2006). Three-day mean wind speeds during our period of study varied between 2.8 and 17.4 m s^{-1}. De Jonge and Beukesom (1995) found that resuspension of MPB increased at mean wind speeds between 4 and 6 m s^{-1}, well within the mean wind speeds we determined in all 3 months. Booth et al. (2000) reported that wave energy induced more than 80%, and approximately 50%, of bottom sediments resuspension when the wind speeds were higher than 10 m s^{-1} and 4 m s^{-1} respectively. The changing depth of overlying water during the immersion period is important in determining the impact of the sediment bed (De Jonge and Van Beusekom, 1995). Wave heights on upper shores in areas of open mudflat and marsh on the U.K. Essex coast are between 0.2 and 0.3 m (Möller and Spencer, 2002) and can propagate energy through the water column, especially during shallow water cover neap tides, thus leading to increased sediment and MPB resuspension.(Green and Coco, 2014). Wind-generated waves have been shown to be more important in enhancing sediment resuspension over mudflats that tidal or wind-drive currents in the Westerschelde, Netherlands (Callaghan et al., 2010).

4.3. Biostabilisation potential by MPB biofilms

There is evidence of biostabilisation in the negative relationships between the MPB biomass (Chl *a* and EPS concentrations) on the sediment and in suspended sediment loads and Chl *a* in the water column (Fig. 5 & Table 3). This further explained by the significant negative correlation between the accumulative sun hours for three days, benthic Chl. *a* and benthic EPS with PC 1 (Table 3). The presence of high MPB biomass (Chl. *a* and EPS concentrations) on the Fingringhoe tidal flat was associated with reduced sediment and MPB ($SS_{Chl. a}$) resuspension (Fig. 5, Table 3). Brito et al. (2012), reported a significant negative relationship between MPB biomass concentration on the sediment surface and phytoplankton biomass in water column in Ria Formosa Lagoon, Portugal, and in the Venice Lagoon, Italy. Higher sediment MPB biomass results in higher EPS concentrations on the sediment surface, potentially decreased the effect of MPB 'wash away' by stabilising the biofilm (Delgado et al., 1991; Austen et al., 1999; Hanlon et al., 2006). The lower SS and $SS_{Chl a}$ on the mud flat than the transition zone may be the result of biostabilisation by MPB (Saint-Béat et al., 2014), with significantly higher sediment EPS concentration on the mud flat than the transition zone. MPB produced EPS that combines with other extra cellular carbohydrate, to form mucilage component on the intertidal biofilms (Underwood and Paterson, 2003). These sticky polysaccharide substances are able to decrease the resuspension of sediment by holding the sediment biofilm together (Blanchard and Forster, 2006) as EPS controls the biostabilisation of sediment in the biofilm (Ubertini et al., 2012, 2015).

Rainfall for three days (sum of rainfall) was responsible to reduce the MPB biomass on the sediment surface during emersion periods (explained by PC2, Fig. 5). Higher rainfall in October 2013, associated with low sum of sun hours will have resulted in less MPB productivity (Wolfstein et al., 2000; Costa et al., 2002; Woelfel et al., 2007; Ha et al., 2018), resulting in reductions in MPB biomass at the sediment surface (Rasmussen et al., 1983) and reduction in bio-stabilisation potential. Field observations and simulated rainfall experiments have been shown to reduce surface sediment critical shear strength, and also reduce, by wash away, the concentrations of sediment Chl *a* and colloidal carbohydrates (Tolhurst et al. 2006, 2008). We found that rainfall had a positive coefficient score in the regression model for SS, but a negative coefficient score for $SS_{Chl. a}$ (Table 2). One interpretation of this could be that benthic diatoms migrated down into the sediments (Underwood and Kromkamp 1999) in response to rainfall, so that they were not present in the surface sediment layers to be resuspended. The lower benthic Chl *a* concentrations in October 2013 corresponded with lower suspended Chl *a* concentrations in the water column, despite high SS loads, because the wetter and less sunny periods at that time meant there was less available MPB on the sediment surface to be resuspended

during immersion (Table 2, Table 3).

5. Summary

There was a relationship between the quantity of MPB on mudflats and the degree of sediment resuspension and movement across the mudflat – transition zone. On the mud flat and the transition zone, 'sum of sun hours' increased Chl. *a* and EPS concentrations, and higher MPB biomass was associated with reduced MPB sediment-water column exchanges. Rainfall was associated with reduced MPB biomass on the intertidal flats, prolonged rainfall increasing the wash away of MPB from sediment surfaces during emersion periods, therefore reduced the ability of MPB biofilms to biostabilise sediment surfaces. Sediment and biofilm resuspension was positively related to wind-induced wave energy. Using MPB diatom species composition as a biological marker demonstrated clear differences in the origin of suspended sediment loads, with the lower suspended solid load during Spring tides associated with coastal phytoplankton taxa, indicating an offshore origin, while benthic diatom assemblages present on the adjacent mudflats were strongly associated with increased sediment loads during neap tides. Contrary to our original hypothesis, both sediment resuspension and sediment deposition were higher during neap tides, which indicates that wave-induced sediment movements during neap tide are more important in redistributing sediment and biofilm material across mudflat profiles in relatively sheltered estuaries.

Funding

Declaration of competing interest

The authors declare that they have no known competing financial interests or personal relationships that could have appeared to influence the work reported in this paper.

Appendix A. Supplementary data

Supplementary data to this article can be found online at https://doi.org/10.1016/j.ecss.2021.107190.

References

Austen, I., Andersen, T.J., Edelvang, K., 1999. The influence of benthic diatoms and invertebrates on the erodibility of an intertidal a mudflat, the Danish Wadden Sea. Estuar. Coast Shelf Sci. 49, 99–111.

Azovsky, A.I., Chertoprood, E.S., Saburova, M.A., Polikarpov, I.G., 2004. Spatio-temporal variability of micro- and meiobenthic communities in a White Sea intertidal sandflat. Estuar. Coast Shelf Sci. 60 (4), 663–671.

Bellinger, B.J., Underwood, G.J.C., Ziegler, S.E., Gretz, M.R., 2009. Aquat. Microb. Ecol. 55, 169–187. https://doi.org/10.3354/ame01287, 169.

Benyoucef, I., Blandin, E., Lerouxel, A., Jesus, B., Rosa, P., Méléder, V., Launeau, P., Barillé, L., 2013. Microphytobenthos interannual variations in a north-European estuary (Loire estuary, France) detected by visible-infrared multispectral remote sensing. Estuar. Coast Shelf Sci. 136, 43–52. https://doi.org/10.1016/j.ecss.2013.11.007.

Benyoucef, I., Blandin, E., Lerouxel, A., Jesus, B., Rosa, P., Meleder, V., Launeau, P., Berille, L., 2014. Microphytobenthos interannual variations in a North European estuary (Loire Estuary, France) detected by visible infrared multispectral remote sensing. Estuar. Coast Shelf Sci. 136, 43–52.

Blanchard, G.F, Agion, T, Guarini, J.M., Herlory, O, Richard, P, 2006. Analysis of the short term dynamics of microphytobenthos biomass on intertidal mudflats. In: Kromkamp, J.C., de Brower, J.F.C., Blanchard, G.F., Forster, R.M., Creach, V., et al. (Eds.), Functioning of microphytobenthos in estuaries. Royal Netherlnads Academy of Arts and Sciences, The Netherlands, pp. 85–97.

Blanchard, G.F., Forster, R.M., 2006. Functioning of microphytobenthos in estuaries. In: Proceedings of the Microphytobenthos Symposium. Amsterdam, Netherlands.

Blanchard, F, Guarini, J, Orvain, F, Sauriau, P, 2001. Dynamic behaviour of benthic microalgal biomass in intertidal mudflats. Mar. Biol. Assoc. U. K. 82, 85–100.

Booth, J.G., Miller, R.L., McKee, B.A., Leathers, R.A., 2000. Wind-induced bottom sediment resuspension in a microtidal coastal environment. Continent. Shelf Res. 20, 785–806. https://doi.org/10.1016/S0278-4343(00)00002-9.

Booty, J.M., Underwood, G.J.C., Parris, A., Davies, R.G., Tolhurst, T.J., 2020. Wading birds affect ecosystem functioning on an intertidal mudflat. Front. Mar. Sci. 7, 685.

Brito, A.C., Fernandes, T.F., Newton, A., Facca, C., Tett, P., 2012. Does microphytobenthos resuspension influence phytoplankton in shallow systems? A comparison through a Fourier series analysis. Estuar. Coast Shelf Sci. 110, 77–84. https://doi.org/10.1016/j.ecss.2012.03.028.

Callaghan, D.P., Bouma, T.J., Klaassen, P., van der Wal, D., Stive, M.J.F., Herman, P.M.J., 2010. Hydrodynamic forcing on salt-marsh development: distinguishing the relative importance of waves and tidal flows. Estuar. Coast Shelf Sci. 89 (1), 73–88. https://doi.org/10.1016/j.ecss.2010.05.013.

Chesman, B.S., Burt, G.R., Langston, W.J., 2006. Characterisation of European marine sites: Essex estuaries, European marine site. Mar. Biol. Assoc. 1–208.

Christie, M.C., Dyer, K.R., 1998. Measurements of the turbid tidal edge over the Skeffling mudflats. Geol. Soc. London 139, 45–55. https://doi.org/10.1144/GSL.SP.1998.139.01.04.

Costa, F.E.P., Brotas, V., Cancela Da Fonseca, L., 2002. Physical characterisation and microphytobenthos biomass of estuarine and lagoon environments of the Southwest coast of Portugal. Limnética 21, 69–80.

Daggers, T.D., Herman, P.M.J., van der wal, D., 2020. Seasonal and spatial variability in patchiness of microphytobenthos on intertidal flats from sentinel-2 satellite imagery. Front. Mar. Sci. 7, 392.

De Jonge, V.N., Van Beusekom, J.E.E., 1995. Wind- and tide-induced resuspension of sediment and microphytobenthos from tidal flats in the Ems estuary. Limnol. Oceanogr. 40, 776–778.

De Jonge, V.N., De Boer, W.F., De Jong, D.J., Brauer, V.S., 2012. Long-term mean annual microphytobenthos chlorophyll a variation correlates with air temperature. Mar. Ecol. Prog. Ser. 468, 43–56. https://doi.org/10.3354/meps09954.

Delgado, M., de Jonge, V.N., Peletier, H., 1991. Experiments on resuspension of naturalmicrophytobenthos populations. Mar. Biol. 108, 321–328.

Easley, J.T., Hymel, S.N., Plante, C.J., 2005. Temporal patterns of benthic microalgal migration on a semi-protected beach. Estuar. Coast Shelf Sci. 64, 486–496. https://doi.org/10.1016/j.ecss.2005.03.013.

Facca, C., Sfriso, A., Socal, G., 2002. Changes in abundance and composition of phytoplankton and microphytobenthos due to increased sediment fluxes in the Venice lagoon, Italy. Estuar. Coast Shelf Sci. 54, 773–792. https://doi.org/10.1006/ecss.2001.0848.

Forster, R.M., Sabbe, K., Vyverman, W., Stal, L.J., 2006. Biodiversity-ecosystem function relationship in microphytobenthic diatoms of the Waterschelde estuary. Mar. Ecol. Prog. Ser. 311, 191–201.

French, R., Spencer, T., 1993. Dynamics of sedimentation in a tide-dominated backbarrier salt marsh, Norfolk , UK. Mar. Geol. 110, 315–331.

Green, M., Coco, G., 2014. Review of wave-driven sediment resuspension and transport in estuaries. Rev. Geophys. 52, 77–117. https://doi.org/10.1002/2013RG000437.

Ha, H.J., Kim, H., Noh, J., Ha, H.K., Khim, J.S., 2018. Rainfall effects on the erodibility of sediment and microphytobenthos in the intertidal flat. Environ. Pollut. 242, 2051–2058. https://doi.org/10.1016/j.envpol.2018.06.079.

Hagerthey, S.E., Defew, E.C., Paterson, D.M., 2002. Influence of *Corophium volutator* and *Hydrobia ulvae* on intertidal benthic diatom assemblages under different nutrient and temperature regimes. Mar. Ecol. Prog. Ser. 245, 47–59. https://doi.org/10.3354/meps245047.

Hanlon, A.R.M., Bellinger, B., Haynes, K., Xiao, G., Hofmann, T.A., Gretz, M.R., Underwood, G.J.C., 2006. Dynamics of extracellular polymeric substance (EPS) production and loss in an estuarine, diatom-dominated, microalgal biofilm over a tidal emersion-immersion period. Limnol. Oceanogr. 51 (1), 79–93.

Hill-Spanik, K.M., Smith, A.S., Plante, C.J., 2019. Recovery of benthic microalgal biomass and community structure following beach renourishment at Folly Beach, South Carolina. Estuar. Coast 42, 157–172.

Hope, J.A., Malarkey, J., Baas, J.H., Peakall, J., Parsons, D.R., Manning, A.J., Bass, S.J., Lichtman, I.D., Thorne, P.D., Ye, L., Paterson, D.M., 2020. Interactions between sediment microbial ecology and physical dynamics drive heterogeneity in contextually similar depositional system. Limnol. Oceanogr. 9999, 1–17. https://doi.org/10.1002/lno.11461.

Koh, C.H., Jong, S.K., Araki, H., Yamanishi, H., Mogi, H., Koga, K., 2006. Tidal resuspension of microphytobenthic chlorophyll a in a Nanaura mudflat, Saga, Ariake Sea, Japan: flood-ebb and spring-neap variations. Mar. Ecol. Prog. Ser. 312, 85–100.

Kovach, W.L., 1999. A Multivariate Statistical Package. Kovach Computing Services, Anglesey, Wales.

Launeau, P., Méléder, V., Verpoorter, C., Barillé, L., Kazemipour-Ricci, F., Giraud, M., Jesus, B., Menn, E. Le, 2018. Microphytobenthos biomass and diversity mapping at different spatial scales with a hyperspectral optical model. Rem. Sens. 10 (5), 1–24. https://doi.org/10.3390/rs10050716.

Lê, S., Josse, J., Husson, F., 2008. FactoMineR: an R package for multivariate analysis. J. Stat. Software 25 (1), 1–18.

Lorenzen, C.J., 1997. Determination ofchlorophyll and pheo-pigments: Spectrophotometricequations. Limnol. Oceanogr. 12, 343–346.

Maunder, J., Paterson, D.M., 2015. Coastal Biodiversity and Ecosystem Service Sustainability (CBESS) surface sediment water content in saltmarsh and mudflat habitats. https://doi.org/10.5285/5ffbc89e-ebed-4fdc-9563-bad42f50e8ce.

McMellor, S., Underwood, G.J.C., 2014. Water policy effectiveness: 30 years of change in the hypernutrified Colne estuary, England. Mar. Pollut. Bull. 81, 200–209.

Mitchell, S.B., Couperthwaite, J.S., West, J.R., Lawler, D.M., 2003. Measuring sedimentexchange rates on Intertidal bank at Blacktoft, Humber estuary, UK. Sci. Total Environ. 535–549.

Möller, I., Spencer, T., 2002. Wave dissipation over macro-tidal saltmarshes: effects of marsh edge typology and vegetation change. J. Coast Res. 36, 506–521. https://doi.org/10.2112/1551-5036-36.sp1.506.

Nedwell, D.B., Underwood, G.J.C., McGenity, T.J., Whitby, C., Dumbrell, A.J., 2016. The Colne Estuary: a long-term microbial ecology observation. Adv. Ecol. Res. 55, 227–281.

Oksanen, J., Blanchet, G., Friendly, M., Kindt, R., Legendre, P., McGlinn, D., Minchin, P. R., O'Hara, R.B., Simpson, G.L., Solymos, P., Stevens, M.H.H., Szoecs, E., Wagner, H., 2019. Vegan: community ecology package. R package version 2.5-6. https://CRAN.R-project.org/package=vegan.

Orvain, F., Sauriau, P.-G., Sygut, A., Joassard, L., 2004a. Interacting effects of *Hydrobia ulvae* bioturbation and microphytobenthos on the erodibility of mudflat sediments. Mar. Ecol. Prog. Ser. 278, 205–223.

Orvain, F., Sauriau, P.G., Sygut, A., Joassard, L., Le Hir, P., 2004b. Interacting effects of *Hydrobia ulvae* bioturbation and microphytobenthos on the erodability of mudflat sediments. Mar. Ecol. Prog. Ser. 278, 205–223. https://doi.org/10.3354/meps278205.

Orvain, F., Sauriau, P.-G., Bacher, C., Prineau, M., 2006. The influence of sediment cohesiveness on bioturbation effects due to *Hydrobia ulvae* on the initial erosion of intertidal sediments: a study combining flume and model approaches. J. Sea Res. 55 (1), 54–73. https://doi.org/10.1016/j.seares.2005.10.002.

Orvain, F., Lefebvre, S., Montepini, J., Sébire, M., Gangnery, A., Sylvand, B., 2012. Spatial and temporal interaction between sediment and microphytobenthos in a temperate estuarine macro-intertidal bay. Mar. Ecol. Prog. Ser. 458, 53–68. https://doi.org/10.3354/meps09698.

Paterson, D.M., 1989. Short-term changes in the erodibility of intertidal cohesive sediments related to the migratory behavior of epipelic diatoms. Limnol. Oceanogr. 34, 223–234. https://doi.org/10.4319/lo.1989.34.1.0223.

Plante, C., Fleer, V., Jones, M.L., 2016. Neutral processes and species sorting in benthic microalgal community assembly: effects of tidal resuspension. J. Phycol. 52, 827–839.

R Core Team, 2020. R: A Language and Environment for Statistical Computing. R Foundation for Statistical Computing, Vienna, Austria. http://www.R-project.org/.

Rakotomalala, C., Guizien, K., Grangeré, K., Lefebvre, S., Dupuy, C., Orvain, F., 2019. Modelling the functioning of a coupled microphytobenthic-EPS-bacterial system in intertidal mudflats. Mar. Environ. Res. 150, 104754. https://doi.org/10.1016/j.marenvres.2019.104754, 2019.

Rasmussen, M.B., Henriksen, K., Jensen, A., 1983. Possible causes of temporal fluctuations in primary production of the microphytobenthos in the Danish Wadden Sea. Mar. Biol. 73, 109–114.

Redzuan, N.S., Underwood, G.J.C., 2020. Movement of microphytobenthos and sediment between mudflats and salt marsh during spring tides. Front. Mar. Sci. 7 https://doi.org/10.3389/fmars.2020.00496.

Ribeiro, L., Brotas, V., Rincé, Y., Jesus, B., 2013. Structure and diversity of intertidal benthic diatom assemblages in contrasting shores: a case study from the tagus estuary. J. Phycol. 49, 258–270. https://doi.org/10.1111/jpy.12031.

Sahan, E., Sabbe, K., Creach, V., Hernandez-Raquet, G., Vyverman, W., Stal, L.J., Muyzer, G., 2007. Community structure and seasonal dynamics of diatom biofilms and associated grazers in intertidal mudflats. Aquat. Microb. Ecol. 47, 253–266. https://doi.org/10.3354/ame047253.

Saint-Béat, B., Dupuy, C., Agogué, H., Carpentier, A., Chalumeau, J., Como, S., David, V., De Crignis, M., Duchêne, J.C., Fontaine, C., Feunteun, E., Guizien, K., Hartmann, H., Lavaud, J., Lefebvre, S., Lefrançois, C., Mallet, C., Montanié, H., Mouget, J.L., Orvain, F., Ory, P., Pascal, P.Y., Radenac, G., Richard, P., Vézina, A.F., Niquil, N., 2014. How does the resuspension of the biofilm alter the functioning of the benthos-pelagos coupled food web of a bare mudflat in Marennes-Oléron Bay (NE Atlantic)? J. Sea Res. 92, 144–157. https://doi.org/10.1016/j.seares.2014.02.003.

Savelli, R., Dupuy, C., Barille, L., Lerouxel, A., Guizien, K., Philippe, A., Bocher, P., Polsenaere, P., Le Fouest, V., 2018. On biotic and abiotic drivers of the microphytobenthos seasonal cycle in a temperate intertidal mudflat: a modelling study. Biogeosciences 15, 7243–7271.

Savelli, R., Bertin, X., Orvain, F., Gernez, P., Dale, A., Coulombier, T., 2019. Impact of chronic and massive resuspension mechanisms on the microphytobenthos dynamics in a temperate intertidal mudflat. J. Geophys. Res. 124, 3752–3777.

Spilmont, N., Seuront, L., Meziane, T., Welsh, D.T., 2011. There's more to the picture than meets the eye: sampling microphytobenthos in a heterogeneous environment. Estuar. Coast Shelf Sci. 95 (4), 470–476. https://doi.org/10.1016/j.ecss.2011.10.021.

Taylor, J.D., McKew, B.A., Kuhl, A., McGenity, T.J., Underwood, G.J.C., 2013. Microphytobenthic extracellular polymeric substances (EPS) in intertidal sediments fuel both generalist specialist EPS-degrading bacteria. Limnol. Oceanogr. 58 (4), 1463–1480. https://doi.org/10.4319/lo.2013.58.4.1463.

Thornton, D.C.O., Dong, L.F., Underwood, G.J.C., Nedwell, D.B., 2002. Factors affecting microphytobenthic biomass, species composition and production in the Colne Estuary (UK). Aquat. Microb. Ecol. 27, 285–300.

Tolhurst, T.J., Jesus, B., Brotas, V., Paterson, D.M., 2003. Diatom migration and sediment armouring - an example from the Tagus Estuary, Portugal. Hydrobiologia 503, 183–193. https://doi.org/10.1023/B:HYDR.0000008474.33782.d.

Tolhurst, T.J., Defew, E.C., De Brouwer, J.F.C., Wolfstein, K., Stal, L.J., Paterson, D.M., 2006. Small-scale temporal and spatial variability in the erosion threshold and properties of cohesive intertidal sediments. Continent. Shelf Res. 26 (3), 351–362. https://doi.org/10.1016/j.csr.2005.11.007.

Tolhurst, T.J., Consalvey, M., Paterson, D.M., 2008. Changes in cohesive sediment properties associated with the growth of a diatom biofilm. Hydrobiologia 596 (1), 225–239. https://doi.org/10.1007/s10750-007-9099-9.

Tomas, C.R., 1997. Identifying marine phytoplankton. Academic Press, San Diego. https://doi.org/10.1016/B978-012693018-4/50010-0.

Ubertini, M., Lefebvre, S., Gangnery, A., Grangeré, K., Le Gendre, R., Orvain, F., 2012. Spatial variability of benthic-pelagic coupling in an estuary ecosystem: consequences for microphytobenthos resuspension phenomenon. PLoS One 7, e44155. https://doi.org/10.1371/journal.pone.0044155.

Ubertini, M., Lefebvre, S., Rakotomalala, C., Orvain, F., 2015. Impact of sediment grain-size and biofilm age on microphytobenthos resuspension. J. Exp. Mar. Biol. Ecol. 467, 52–64. https://doi.org/10.1016/j.jembe.2015.02.007.

Underwood, G.J.C., 1994. Seasonal and spatial variation n epipelic diatom assemblages in the Severn estuary. Diatom Res. 9, 451–472.

Underwood J, C., G, Hanlon, A.R.M., Oxborough, K, Baker, N.R., et al., 2005. Species-specific variation in migratory rhythms and photosynthetic efficiency in mixed-species biofilms. Am. Soc. Limnol. Oceanogr. 50 (3), 755–767.

Underwood, G.J.C., Kromkamp, J., 1999. Primary production by phytoplankton and microphytobenthos in estuaries. Adv. Ecol. Res. 29, 93–153.

Underwood, G.J.C., Paterson, D.M., 1993. Recovery of intertidal benthic diatoms after biocide treatment and associated sediment dynamics. Journal of the Marine Biological Association of the UK 73, 25–45.

Underwood, G.J.C., Paterson, D.M., 2003. The Importance of Extracellular Carbohydrate Production by Marine Epipelic Diatoms. Elsevier Academic Press. https://books.google.com.my/books?id=2VnbYgEACAAJ.

Underwood, G.J.C., Phillips, J., Saunders, K., 1998. Distribution of estuarine benthic diatom species along salinity and nutrient gradients. Eur. J. Phycol. 33, 173–183. https://doi.org/10.1080/09670269810001736673.

van der Wal, D., Wielemaker-van den Dool, A., Herman, P.M.J., 2010. Spatial synchrony in intertidal benthic algal biomass in temperate coastal and estuarine ecosystems. Ecosystems 13, 338–351. https://doi.org/10.1007/s10021-010-9322-9.

Weerman, E.J., Herman, P.M.J., Van De Koppel, J., et al., 2011. Top down control inhibits spatial self-organization of a patterned landscape. Ecol. Soc. Am. 92 (2), 487–495.

Weerman, E.J., Van Belzen, J., Rietkerk, M., Temmerman, S., Kéfi, S., Herman, P.M.J., Van De Koppel, J., 2012. Changes in diatom patch-size distribution and degradation in a spatially self-organized intertidal mudflat ecosystem. Ecology 93, 608–618.

Witkowski, A., Lange-Bertalot, H., Metzeltin, D., 2000. Diatom Flora of Marine Coasts. Iconographia Diatomologica V. 7. Ganter, Ruggell. Koeltz Scientific Books, Königstein, Germany.

Woelfel, J., Schumann, R., Adler, S., Hubener, T., Karsten, U., 2007. Diatoms inhabiting a wind flat of the Baltic Sea: Species diversity and seasonal succession. Estuar. Coast Shelf Sci. 75 (3), 296–307.

Wolfstein, K., Colijn, F., Doerffer, R., 2000. Seasonal dynamics of microphytobenthos biomass and photosynthetic characteristics in the northern German Wadden sea, obtained by the photosynthetic light dispensation system. Estuar. Coast Shelf Sci. 51, 651–662.

Wood, C.L., Hawkins, S.J., Godbold, J.A., Solan, M., 2015a. Coastal Biodiversity and ecosystem service sustainability (CBESS) total organic carbon in mudflat and saltmarsh habitats. NERC environmental information data centre. https://doi.org/10.5285/d4e9f0f7-637a-4aa4-b9df-2a4ca5bfaded.

Wood, C.L., Hawkins, S.J., Godbold, J.A., Solan, M., 2015b. Coastal Biodiversity and Ecosystem Service Sustainability (CBESS) macrofaunal abundance in mudflat and saltmarsh habitats. NERC Environmental Information Data Centre. https://doi.org/10.5285/d5317679-449f-4829-9caf-39973fe27c07.

Zhu, Z., van Belzen, J., Zhu, Q., van de Koppel, J., Bouma, T.J., 2019. Vegetation recovery on neighboring tidal flats forms an Achilles' heel of saltmarsh resilience to sea level rise. Limnol. Oceanogr. 9999, 1–12. https://doi.org/10.1002/lno.11249.